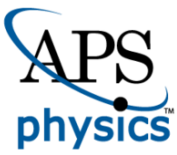

Biomechanical Feedback Strengthens Jammed Cellular Packings

Pawel Gniewek, Carl F. Schreck, and Oskar Hallatschek

Phys. Rev. Lett. **122**, 208102 — Published 22 May 2019

DOI: 10.1103/PhysRevLett.122.208102

Biomechanical feedback strengthens jammed cellular packings

Pawel Gniewek,* Carl F. Schreck,† and Oskar Hallatschek‡
Departments of Physics and Integrative Biology, University of California Berkeley, USA 94720

Growth in confined spaces can drive cellular populations through a jamming transition from a fluid-like state to a solid-like state. Experiments have found that jammed budding yeast populations can build up extreme compressive pressures (over 1MPa), which in turn feed back onto cellular physiology by slowing or even stalling cell growth. Using numerical simulations, we investigate how this feedback impacts the mechanical properties of model jammed cell populations. We find that feedback directs growth toward poorly-coordinated regions, resulting in an excess number of cell-cell contacts that rigidify cell packings. Cell packings posses anomalously large shear and bulk moduli that depend sensitively on the strength of feedback. These results demonstrate that mechanical feedback on the single-cell level is a simple mechanism by which living systems may tune their population-level mechanical properties.

Granular materials undergo a jamming transition upon compression, at which point the entire system becomes rigid so that further compaction is not possible without pressure build-up [1, 2]. Packings obtained in this manner are spatially-disordered similar to liquids but, like solids, do not yield (irreversibly deform) upon application of an external stress [3]. The transition occurs at a well-defined packing fraction $\phi = \phi_J$ [2], at which the system is marginally stable (*i.e.* removing a single contact causes the system to lose mechanical rigidity) [4]. Compression beyond the jamming point ($\phi > \phi_J$) rigidifies packings, resulting in mechanical properties that exhibit nontrivial power law scalings as a function of $\delta\phi = \phi - \phi_J$ [2, 4–8]. It has been recently demonstrated that confined microbial populations can similarly drive themselves into a rigid state via cellular growth and division [9]. Cellular populations fundamentally differ from inert granular media in that, whereas granular systems are static unless driven externally [10–15], cellular populations are active systems that are driven internally as cells consume energy from their environments in order to move or grow [9, 16–21]. Growth-driven jamming also differs from the recently studied motility-driven jamming transition [18, 22], in which the system is kept at constant density and is driven by innate cell motility rather than growth. In the case of growth-driven jamming, it is an open question if the cellular packings have the same universal physical properties as conventional granular materials [2, 7]. In particular, experiments have shown that cell-cell forces slow down cell growth [9], but it remains unknown whether this mechanical feedback at the single-cell level has consequences for population-level mechanical properties. In this work, we show that budding cells can control the mechanical properties of densely-packed populations by leveraging their shape and the coupling between cellular growth rate and cell-cell forces [9, 23].

We perform 2D numerical simulations of budding yeast populations growing in space-limited environments. Each cell is represented as conjoined mother and daughter lobes that reproduce asexually via expansion of the daughter "bud" (Fig. 1(a)), a modeling approach first developed in [9] alongside microfluidic experiments. In this mode of proliferation, bud expansion progresses until the bud reaches the size of a mother cell, at which point the bud detaches and mother and bud form two new cells. To capture the experimentally-measured diminished growth rate under compressive mechanical stress [9], each cell in our model grows at a rate γ that decreases exponentially with the pressure exerted on its daughter bud P_{bud}: $\gamma \propto e^{-P_{\text{bud}}/P_0}$ (Fig. 1(b)). The feedback pressure P_0 controls the strength of feedback, with smaller values of P_0 corresponding to "stronger" feedback.

As cells proliferate, repulsive elastic forces between cells (see Supplemental Material, Fig. S1) push the population to expand outward via completely over-damped dynamics (Fig. 1(c)-(g)). In the absence of external confinement (Fig. 1(c) and (d)), the population remains at zero pressure with no force-bearing contacts between cells. However once the population fills the environment in which it resides (implemented here via periodic boundary conditions), it is driven through a jamming transition (Fig. 1(e)) at packing fraction $\phi_J \approx 0.84$ that is characterized by a sudden increase in the population pressure P (Fig. 1(h)) and a discontinuous jump in the number of contacts Z (Fig. 1(i)). While mechanical feedback does not affect packings below jamming, feedback strength P_0 determines how pressure and contacts build up beyond jamming. To understand how mechanical rigidity emerges beyond jamming we first investigate mechanisms underlying the creation of new cell-cell contacts, since contacts are known to control the mechanical properties of non-living granular media [2, 7, 24].

At the jamming point, the average number of contacts per cell jumps from $Z = 0$ to $Z = Z_J \approx 5.5$ (Fig. 1(i)), a result that is independent of P_0. The value $Z_J \approx 5.5$ is smaller than the naive *isostatic* expectation $Z_{\text{iso}}^{\text{naive}} = 6$, predicted by the Maxwell criterion by equating the number of bud-bud contacts per cell ($Z_{\text{iso}}^{\text{naive}}/2$) to the number of degrees of freedom per cell (3: two translational and one rotational) [25]. This deviation from naive isostaticity results from the presence of numerous cells whose buds are not in contact with their neighbors (depicted

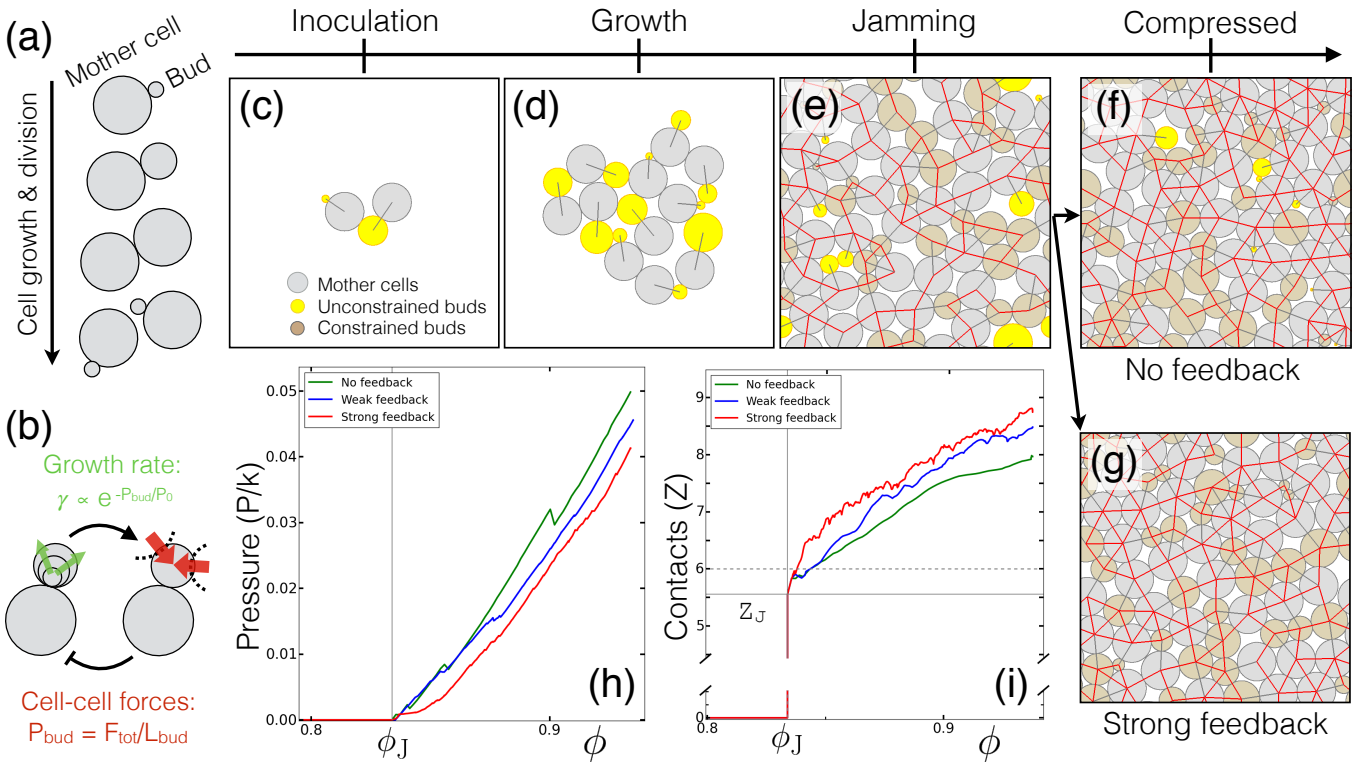

FIG. 1. (a) Schematic of the growth and division process. Each cell grows by bud expansion. Budding culminates via mother-daughter separation when the daughter reaches the size of a mother cell. (b) Schematic of feedback of cell-cell forces onto growth. Daughter buds contact their neighbors as they grow (dashed black lines). The associated contact forces generate pressure on the growing bud, defined here as the ratio of total force magnitude $F_{\rm tot}$ to perimeter $L_{\rm bud}$ of the daughter bud (see Supplemental Material): $P_{\rm bud} = F_{\rm tot}/L_{\rm bud}$. This pressure in turn decreases its growth rate as $\gamma \propto e^{-P_{\rm bud}/P_0}$. (c-g) Snapshots from a typical simulation. (c) Each simulation is inoculated with two cells. (d) Cell growth drives the population to expand outward. During expansion, cells interact with their neighbors via repulsive elastic forces and completely overdamped dynamics. (e) The population undergoes a "jamming transition" at $\phi_J = 0.84$, at which point a system-spanning network of force-bearing intercellular contacts develops (red lines). At jamming, most mother (gray) and daughter (brown) buds are constrained by their neighbors, but $\approx 25\%$ of buds (yellow) are unconstrained (see Supplemental Material). Above jamming, packings have more unconstrained buds when (f) cell growth rate is independent of mechanical pressure than when (g) pressure feeds back onto growth ($P_0/k = 10^{-3}$). Both (f) and (g) are at $\phi = 0.89$. (h) The pressure that the entire population exerts on its surroundings (see Supplemental Material) is zero below jamming ($\phi < \phi_J$) and increases as the cells grow above jamming ($\phi > \phi_J$). With no feedback and weak feedback ($P_0/k = 5 \times 10^{-3}$), P is almost linear in ϕ. For strong feedback ($P_0/k = 10^{-3}$), P increases more slowly with ϕ. All pressures are measured in units of the cell-cell modulus k (see Supplemental Material). (i) The number of contacts Z per cell jumps discontinuously from $Z \approx 0$ to $Z = Z_J \approx 5.5$ at jamming at ϕ_J, and increases more quickly for strong feedback than for weak or no feedback. For periodic boundary conditions, (c)-(g) use box size $L = 7\sigma$ and (h) and (i) use box size $L = 15\sigma$ where σ is a cell diameter. (h) and (i) show data for one typical population. We find that Z_J does not exhibit significant system size effect, with $Z_J \approx 5.5$ for different initial conditions and for large systems (Fig. S2(b)).

in yellow in Fig. 1(e)). Cells with "unconstrained" buds are free to rotate about their mother, and therefore correspond to degrees of freedom that are not constrained by cell-cell contacts. By subtracting the number of unconstrained buds per cell f_u from the number cellular degrees of freedom, we can derive a modified isostatic criterion $Z_{\rm iso} = Z_{\rm iso}^{\rm naive} - 2f_u$ (see Supplemental Material) that is satisfied by nearly all simulated populations at the $P \to 0$ jamming threshold (Fig. S2(a)). This isostatic criterion can alternatively be derived by considering cells to be composed of two separate lobes, and removing all lobes are are not mechanically stable (Supplemental Material).

We find that a substantial fraction of cells ($f_u \approx 25\%$) have unconstrained buds at jamming, which manifests in a strong departure (Fig. S2) from naive isostaticity ($Z_{\rm iso}^{\rm naive} - Z_J \approx 0.5$). The relationship between unconstrained buds and contacts is also observed in non-growing systems. Packings of asymmetric dumbbell-shaped particles that resemble budding cells yield similar results ($f_u \gtrsim 10\%$ and $Z_{\rm iso}^{\rm naive} - Z_J \gtrsim 0.2$) [26], whereas packings of symmetric dumbbells with equal-sized lobes have many fewer unconstrained buds ($f_u \lesssim 2\%$) and are therefore much closer to isostacity ($Z_{\rm iso}^{\rm naive} - Z_J \lesssim 0.04$) [27]. Packings of other frictionless objects such as

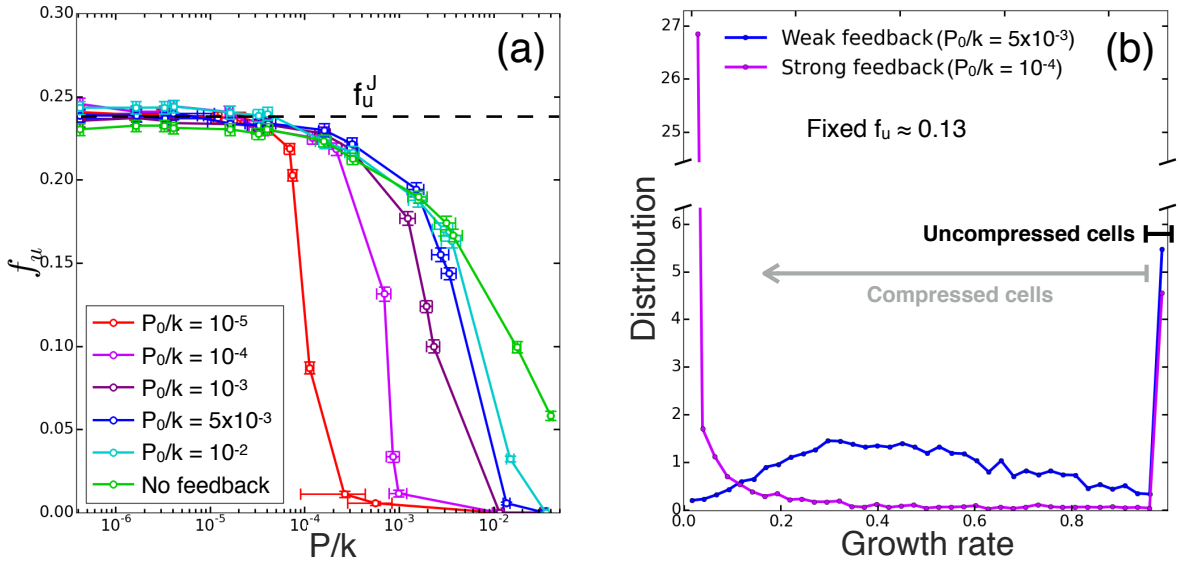

FIG. 2. (a) Fraction of unconstrained buds f_u as a function of the population pressure generated by growing budding yeast packings above the jamming point. f_u^J denotes the value of f_u at the jamming threshold ($P \to 0$). Colored lines correspond to different feedback values. Populations without feedback have a finite number of unconstrained buds up to $P \approx P_{\max}$, which corresponds to $\phi \approx 1$ (Fig. 1(h)). (b) Distribution of cell growth rates for microbial populations with weak ($P_0/k = 5 \times 10^{-3}$) and strong ($P_0/k = 10^{-4}$) feedback. In order to measure growth rates as unconstrained buds make contact, both populations have a value of f_u that is $\approx 50\%$ of that measured at jamming ($f_u \approx 0.13$). The black bar denotes cells under no or very little pressure, thus growing as they would in the absence of feedback. The gray bar denotes cells whose growth rates are reduced by pressure. The growth rate $\gamma(i)$ of each cell is normalized by γ_i^0, the growth rate that a cell would have without feedback (see Supplemental Material). Simulations have box size $L = 15\sigma$. Each data point is averaged over 100 independent inoculations.

ellipsoids [26, 28–30] and spherocylinders [26, 31] also exhibit deviations from naive isostaticity due to unconstrained degrees of freedom. Additionally, a similar phenomena occurs in frictional packings, where the deviation from naive isostaticity can be accounted for by counting the number of sliding contacts [32, 33].

As cells grow beyond the jamming point ($\phi > \phi_J$), the population pressure P builds (Fig. 1(h)) and unconstrained buds begin to make contact with their neighbors (Fig. 1(f)-(g), Fig. 2(a)). This increase in population pressure, corresponding to comparable pressure on individual cells $\langle P_{\rm bud} \rangle \approx P$, triggers mechanical feedback and slows the growth of cells for $P \gtrsim P_0$ (Fig. 1(b)). We observe two distinct behaviors for "strong" ($P_0 \lesssim P_{\rm th}$) and "weak" ($P_0 \gtrsim P_{\rm th}$) feedback, separated by a threshold pressure ($P_{\rm th}/k \approx 0.005$) much smaller than the maximal pressure felt by populations near confluency $\phi \approx 1$ ($P_{\max}/k \approx 0.1$, see Supplemental Material). For weak feedback, cell growth rates are not strongly reduced as unconstrained buds make contact with their neighbors (Fig. 2(b)). On the other hand, strong feedback slows the growth of compressed buds by such an extent that it creates two distinct subpopulations: compressed buds that are effectively stalled in their cell cycle and unconstrained (and therefore uncompressed) buds that are actively growing. The threshold ($P_{\rm th}$) between strong and weak feedback corresponds to the pressure at which the majority of previously unconstrained buds contact their neighbors in the absence of feedback (Fig. 2(a)). Therefore, in contrast to weak feedback where cells are driven into contact by nearly uniform population growth, strong feedback directs growth toward unconstrained buds.

The directed growth of unconstrained buds enables populations growing under strong feedback to create additional contacts with little associated pressure build-up (Fig. 3(a)). In the absence of feedback, the excess number of contacts increases roughly as $\Delta Z = Z - Z_{\rm iso} \propto P^{1/2}$, as expected from studies on jamming in non-living systems [2, 27], where $Z_{\rm iso} = Z_{\rm iso}^{\rm naive} - 2f_u$ increases as unconstrained make contact (Fig. S7). However, populations growing under strong feedback exhibit abrupt departures from this expectation (Fig. 3(a)) at pressures P' that decrease with increasing feedback strength ($P' \propto P_0$). For strong feedback, additional contacts are generated rapidly as a function of P until all unconstrained buds make contact with their neighbors (Fig. 2(a)). These new unconstrained bud contacts result in $Z = {Z_{\rm iso}}^{\rm naive} + 2f_u^J$ and $Z_{\rm iso} = {Z_{\rm iso}}^{\rm naive}$, an excess of $\Delta Z_{\rm u} = 2f_u^J \approx 0.5$ contacts (Fig 3(a), Supplemental Material). Since the excess of contacts is pushed to lower pressures as P_0 decreases, we conjecture that when $P_0 = 0$ (see phenomenological model in Supplemental Material, Fig. S8) cell packings will have more contacts than required for mechanical stability even at $P = 0$ (i.e., *hyperstaticity*).

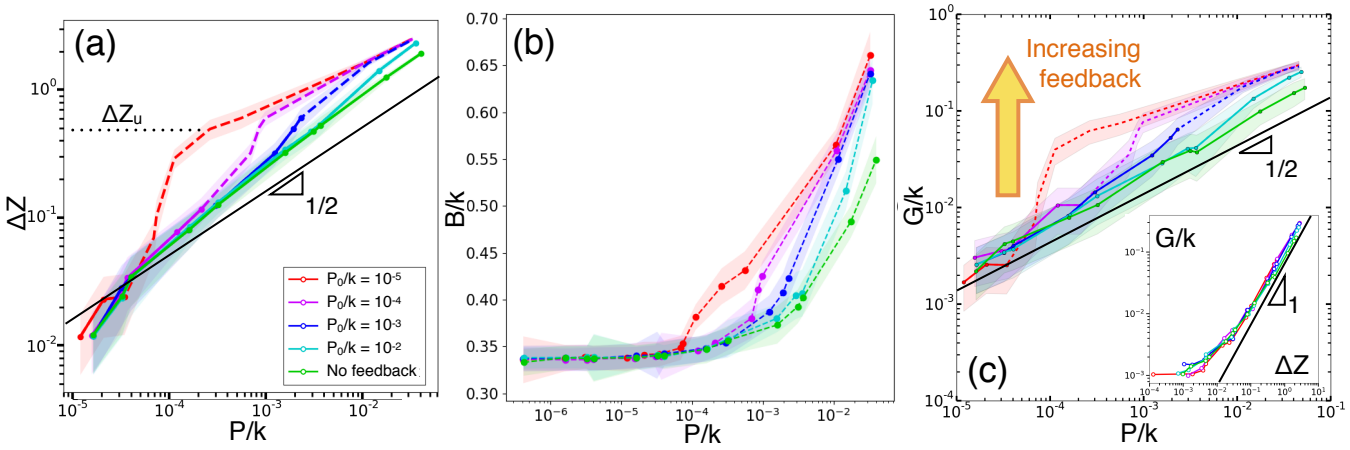

FIG. 3. (a) Excess number of contacts, $\Delta Z = Z - Z_{\rm iso}$. Colored lines correspond to different feedback values and shaded regions represent one standard deviation. To show where growth has been appreciably slowed by cell-cell forces, dashed colored lines correspond to populations whose average cell growth rate is reduced by a factor of 10 compared to growth without feedback (Fig. S5). Solid colored lines correspond to growth rates within a factor of 10 of those without feedback. The dotted black line shows the number of contact resulting from unconstrained bud contacts $\Delta Z_{\rm u} = 2f_u \approx 1$ (see Supplemental Material). (b) Bulk modulus as a function of pressure for populations growing under five different feedback strengths. (c) Shear modulus G for cell packings. Inset: Shear modulus in terms of excess contact number ΔZ. Line-types in (b) are the same as shown in (a). Black lines for each panel show known results for disk packings $G \propto \Delta Z \propto P^{1/2}$ [2]. Simulations have box size $L = 15\sigma$ and each data point is averaged over 100 independent inoculations. For this box size, packing have $\langle N \rangle \approx 172$ cells at the jamming point, for which system size effects in ΔZ and G are expected for smaller pressures ($P/k \ll 1/N^2 \approx 3 \times 10^{-5}$ [24]) than presented here. We do not find significant system size effects in ΔZ (Fig. S2(b)) or G (Fig. S3).

How do excess contacts impact the mechanical properties of populations growing under strong feedback? Since prior studies have found that contacts generated by external compression increase the rigidity of granular packings [2, 34], we hypothesize that contacts generated via bud growth likewise rigidify cell packings. To test this hypothesis, we first measure resistance to external compression as quantified by the bulk modulus $B = \phi_e dP/d\phi_e$, where the packing fraction ϕ_e increases via compaction rather than cell growth. We find that B increases with feedback strength (Fig. 3(b)), a direct consequence of the formation of the additional contacts (Fig. S4). In contrast to the increase in B ($dP/d\phi_e$ increases with P_0), pressure increases more slowly as packing fraction is added via cellular growth ($dP/d\phi$ decreases with P_0 in Fig. 1(h)). Mechanical feedback therefore allows cell populations to disentangle their mechanical response to internal perturbations (cell growth) from their response to external perturbations (external compression).

While the generation of excess contacts only slightly modifies the bulk modulus (B increases by $\leq 20\%$ at fixed pressure), we expect these contacts to substantially impact the shear modulus since non-living packings are known to be fragile with respect to shear [2, 24, 35]. By measuring the shear stress Σ_{xy} generated under simple shear strain γ_{xy} (see Supplemental Material), we find that the shear modulus $G = d\Sigma_{xy}/d\gamma_{xy}$ scales with pressure as $G \propto P^{1/2}$ in the absence of feedback but increases sharply for strong feedback (Fig 3(c)) as unconstrained buds make contact (Fig 2(a)). The sharp increase in G is indeed controlled by contacts made by unconstrained buds, as we find a one-to-one relationship between ΔZ and G (Fig 3(c) inset). The stabilizing role of added contacts can be understood from constraint counting: both Z and $Z_{\rm iso}$ increase as unconstrained buds make contact, but Z increases faster than $Z_{\rm iso}$ so that packings are pushed above isostaticity (see Supplemental Material).

The result $G \propto P^{1/2}$ for growth without feedback, also observed in non-living packings [2, 27], suggests that populations are fragile with respect to shear near jamming and therefore susceptible to fluidization under thermal excitation [35] or cell motility [22]. Populations growing under strong feedback, on the other hand, are stabilized by excess contacts even at very small pressure. Therefore, in contrast to populations without feedback and non-living packings where rigidity comes at a cost of increased cell-cell forces, cell populations growing under strong feedback can rigidify themselves with minimal associated pressure.

We have shown that budding cell populations undergo a growth-driven jamming transition that has mechanical properties not observed in non-living packings. Populations growing under mechanical feedback develop more cell-cell contacts. These contacts are force-bearing and increase the population's resistance to shear and compressive stresses by an amount expected from studies on non-living granular materials [2]. As budding cell populations grow, this creation of excess intercellular contacts

is not accompanied by a faster buildup of the internal pressure in contrast to the anticipated behavior of ordinary granular materials. The aforementioned feedback mechanism is a simple and efficient means for expanding microbial populations to increase their resistance to mechanical stress without building up growth-limiting compressive mechanical forces. Our results could be experimentally tested by measuring the number of bud-bud contacts in a microfluidic setup [9] or measuring the rheological properties via techniques such as rotating disk rheometry [36] or deformable microfluidic devices [37].

The ability to control their mechanical rigidity may have important biologicial consequences for microbial populations, such as preventing fluidization caused by apoptosis [38–41] or cell motility [17, 22], reducing the susceptibility of biofilms to sloughing [42], or regulating biofilm formation under self-induced mechanical stress [43]. Furthermore, bio-insipired mechanical feedback may provide a promising method for creating synthetic materials with tunable mechanical properties.

Acknowledgments. Research support is provided by the Simons Foundation Award No. 327934, NSF Career Award No. 1555330, General Medical Sciences of the NIH Award No. R01GM115851. This work also benefited from the facilities and staff of the National Energy Research Scientific Computing Center, a DOE Office of Science User Facility supported by the Office of Science of the U.S. DOE under Contract No. DE-AC02-05CH11231. We thank Jason Paulose, Marie Duvernoy, and Kyle VanderWerf for their helpful comments.

We note that PG and CFS contributed equally to this work.

* Co-first author; pawel.gniewek@berkeley.edu
† Co-first author; carl.schreck@berkeley.edu
‡ ohallats@berkeley.edu

[1] C. S. O'Hern, S. A. Langer, A. J. Liu, and S. R. Nagel, Phys. Rev. Lett. **88**, 075507 (2002).
[2] C. S. O'Hern, L. E. Silbert, A. J. Liu, and S. R. Nagel, Phys. Rev. E **68**, 011306 (2003).
[3] A. J. Liu and S. R. Nagel, Nature **396**, 21 (1998).
[4] M. Wyart, S. R. Nagel, and T. A. Witten, Eur. Phys. Lett. **72**, 486 (2005).
[5] L. E. Silbert, A. J. Liu, and S. R. Nagel, Phys. Rev. Lett. **95**, 098301 (2005).
[6] L. E. Silbert, A. J. Liu, and S. R. Nagel, Phys. Rev. E **73**, 041304 (2006).
[7] M. Wyart, Annales de Physique **30**, 1 (2005).
[8] W. G. Ellenbroek, E. Somfai, M. van Hecke, and W. van Saarloos, Phys. Rev. Lett. **97**, 258001 (2006).
[9] M. Delarue, J. Hartung, C. Schreck, P. Gniewek, L. Hu, S. Herminghaus, and O. Hallatschek, Nature Physics **12**, 762 (2016).
[10] T. S. Majmudar and R. P. Behringer, Nature **435**, 1079 (2005).
[11] D. Bi, J. Zhang, B. Chakraborty, and R. P. Behringer, Nature **480**, 355 (2011).
[12] C. Heussinger and J.-L. Barrat, Phys. Rev. Lett. **102**, 218303 (2009).
[13] S. Dagois-Bohy, B. P. Tighe, J. Simon, S. Henkes, and M. van Hecke, Phys. Rev. Lett. **109**, 095703 (2012).
[14] N. Iikawa, M. M. Bandi, and H. Katsuragi, Phys. Rev. Lett. **116**, 128001 (2016).
[15] T. Bertrand, R. P. Behringer, B. Chakraborty, C. S. O'Hern, and M. D. Shattuck, Phys. Rev. E **93**, 012901 (2016).
[16] S. Ramaswamy, Annual Review of Condensed Matter Physics **1**, 323 (2010).
[17] D. Bi, J. H. Lopez, J. M. Schwarz, and M. L. Manning, Nature Physics **11**, 1074 (2015).
[18] D. Bi, X. Yang, M. C. Marchetti, and M. L. Manning, Phys. Rev. X **6**, 021011 (2016).
[19] D. Barton, S. Henkes, C. Weijer, and R. Sknepnek, PLoS Comput. Biol. **13**, e1005569 (2017).
[20] F. Giavazzi, M. Paoluzzi, M. Macchi, D. Bi, G. Scita, M. L. Manning, R. Cerbino, and M. C. Marchetti, Soft Matter **14**, 3471 (2018).
[21] A. Fodor and M. C. Marchetti, Physica A **504**, 106 (2018).
[22] S. Henkes, Y. Fily, and M. C. Marchetti, Phys. Rev. E **84**, 040301 (2011).
[23] M. Delarue, G. Poterewicz, O. Hoxha, J. Choi, W. Yoo, J. Kayser, L. Holt, and O. Hallatschek, Proceedings of the National Academy of Sciences **114**, 13465 (2017).
[24] C. P. Goodrich, A. J. Liu, and S. R. Nagel, Phys. Rev. Lett. **109**, 095704 (2012).
[25] S. Alexander, Physics Reports **296**, 65 (1998).
[26] K. VanderWerf, W. Jin, M. D. Shattuck, and C. S. O'Hern, Phys. Rev. E **97**, 012909 (2018).
[27] C. F. Schreck, N. Xu, and C. S. O'Hern, Soft Matter **6**, 2960 (2010).
[28] A. Donev, R. Connelly, F. H. Stillinger, and S. Torquato, Phys. Rev. E **75**, 051304 (2007).
[29] M. Mailman, C. F. Schreck, C. S. O'Hern, and B. Chakraborty, Phys. Rev. Lett. **102**, 255501 (2009).
[30] C. F. Schreck, M. Mailman, B. Chakraborty, and C. S. O'Hern, Phys. Rev. E **85**, 061305 (2012).
[31] S. R. Williams and A. P. Philipse, Phys. Rev. E **67**, 051301 (2003).
[32] K. Shundyak, M. van Hecke, and W. van Saarloos, Phys. Rev. E **75**, 010301 (2007).
[33] S. Henkes, M. van Hecke, and W. van Saarloos, Europhysics letters **90**, 14003 (2010).
[34] W. G. Ellenbroek, E. Somfai, M. van Hecke, and W. van Saarloos, Phys. Rev. Lett. **97**, 258001 (2006).
[35] P. Olsson and S. Teitel, Phys. Rev. Lett. **99**, 178001 (2007).
[36] B. W. Towler, C. J. Rupp, A. B. Cunningham, and S. P, Biofouling **19**, 279 (2003).
[37] D. N. Hohne, J. G. Younger, and M. J. Solomon, Langmuir **25**, 7743 (1009).
[38] J. Ranft, M. Basan, J. Elgeti, J.-F. Joanny, J. Prost, and F. Julicher, Proc. Natl. Acad. Sci. **107**, 20863 (2010).
[39] D. A. Matoz-Fernandez, E. Agoritsas, J.-L. Barrat, E. Bertin, and K. Martens, Phys. Rev. Lett. **118**, 158105 (2017).
[40] S. Jacobeen, J. T. Pentz, E. C. Graba, C. G. Brandys, W. C. Ratcliff, and P. J. Yunker, Nature Physics **14**, 286 (2018).
[41] S. Jacobeen, E. C. Graba, C. G. Brandys, T. C. Day,

W. C. Ratcliff, and P. J. Yunker, Phys. Rev. E **97**, 050401 (2018).
[42] K. J. B., J. Dent. Res. **89** (2010).
[43] C. H. G. A. L. A. Chu E. K., Kilic O., Nature Communications **9** (2010).
[44] P. Gniewek, "Jamming by Growth," DOI: `10.5281/zenodo.2575758` (2019).
[45] W. H. Press, B. P. Flannery, S. A. Teukolsky, and W. T. Vetterling, *Numerical recipes in Fortran* (Cambridge Univ. Press, 1992).
[46] J. Lin and A. Amir, Cell Systems **5**, 358 (2017).
[47] S. D. Talia, J. M. Skotheim, J. M. Bean, E. D. Siggia, and F. R. Cross, Nature **448** (2007).
[48] J. Olafsen, *Experimental and Computational Techniques in Soft Condensed Matter Physics* (Cambridge University Press, 2010) Chap. 2.